Dynamic relaxation of topological defect at Kosterlitz–Thouless phase transition

2011 J. Phys. A: Math. Theor. 44 345005

(http://iopscience.iop.org/1751-8121/44/34/345005)

J. Phys. A: Math. Theor. **44** (2011) 345005 (15pp) doi:10.1088/1751-8113/44/34/345005

Dynamic relaxation of topological defect at Kosterlitz–Thouless phase transition

X P Qin[1,2], **B Zheng**[1] **and N J Zhou**[1]

[1] Department of Physics, Zhejiang University, Hangzhou 310027, People's Republic of China
[2] School of Science, Zhejiang University of Science and Technology, Hangzhou 310023, People's Republic of China

E-mail: zheng@zimp.zju.edu.cn

Received 6 May 2011, in final form 10 July 2011
Published 8 August 2011
Online at stacks.iop.org/JPhysA/44/345005

Abstract
With Monte Carlo methods we study the dynamic relaxation of a vortex state at the Kosterlitz–Thouless phase transition of the two-dimensional *XY* model. A local pseudo-magnetization is introduced to characterize the symmetric structure of the dynamic systems. The dynamic scaling behavior of the pseudo-magnetization and Binder cumulant is carefully analyzed, and the critical exponents are determined. To illustrate the dynamic effect of the topological defect, similar analysis for the dynamic relaxation with a spin-wave initial state is also performed for comparison. We demonstrate that a limited amount of quenched disorder in the core of the vortex state may alter the dynamic universality class. Furthermore, theoretical calculations based on the long-wave approximation are presented.

PACS numbers: 64.60.Ht, 68.35.Rh, 05.10.Ln

(Some figures in this article are in colour only in the electronic version)

1. Introduction

In recent years, many activities have been devoted to the study of dynamic processes far from equilibrium. Compared with spin-glass and structural-glass dynamics, critical dynamics at standard second-order or Kosterlitz–Thouless (KT) phase transitions is relatively simple. One is able to systematically explore the universal dynamic scaling behavior far from equilibrium, up to the *macroscopic* short-time regime [1–4]. Although the spatial correlation length is still short in the beginning of the time evolution, the dynamic scaling form is induced by the divergent correlating time. Based on the short-time dynamic (STD) scaling form, new methods for the determination of both dynamic and static critical exponents as well as the critical temperature have been developed [3–5]. Since the measurements are carried out in the short-time regime, one does not suffer from critical slowing down. Such a dynamic approach is especially useful when one is interested in tackling *both the statics and dynamics* of the critical systems. Recent progress in the short-time critical dynamics includes, for example,

theoretical calculations and numerical simulations of the *XY* models and Josephson junction arrays [6–10], magnets with quenched disorder [11–15], ageing phenomena [16–20], domain-wall (DW) dynamics [21–24], weak first-order phase transitions [25, 26, 11, 27] and various applications and developments [28–35].

In the understanding of the critical dynamics far from equilibrium, the dependence of the dynamic scaling behavior on the *macroscopic* initial condition [1, 3, 36] is essential. Up to now, the dynamic relaxation with disordered and ordered initial states has been systematically investigated [1, 5, 3, 36]. Physically, the disordered and ordered initial states correspond to the states at very high and zero temperatures, respectively. The ordered initial state can also be considered as a state under a strong external magnetic field. Recently, the dynamic relaxation of a DW is also concerned [21, 22], and it shares certain common features with those around free and disordered surfaces [21]. The three relaxation processes above are typical but relatively simple. By these successes, we are encouraged to tackle more general relaxation processes. On the other hand, for strongly disordered systems such as spin glasses, not only the metastable states but also the ground states are not simply ordered and homogeneous, and the standard magnetization does not characterize the relaxation dynamics starting from a zero or low temperature. Methodologically and technically one needs to develop new concepts.

From theoretical view points, metastable states and low-energy excited states may play important roles in phase transitions. One example is the spin-glass transition, and another is the KT transition in the two-dimensional (2D) *XY* model. In the latter case, low-energy excited states such as spin waves destroy the magnetic order, and metastable state such as vortices and vortex pairs dominate the phase transition. Since vortices and vortex pairs are *topological defects*, the KT transition is sometimes called a topological phase transition. The effect of topological defects is often a main issue in the study of phase transitions, also in non-equilibrium dynamics [37]. In fact, one has not achieved too much understanding for the dynamic relaxation of metastable states and low-energy excited states, although its importance is often qualitatively addressed.

Recently, many activities have been devoted to the study of vortex states and vortex structures in nanowires and nanomagnets. Attention is also drawn to the single-vortex state in experiments and numerical simulations [38–42]. For example, a single-vortex structure is explicitly observed in the DW of a ferromagnetic nanowire [40], and a second-order transition between a DW and a vortex state is detected [42]. In [41], the abnormal diffusion of a single vortex in the 2D *XY* model is also numerically simulated. Therefore, the vortex state is a physically important object. In this paper, we numerically and theoretically study the relaxation dynamics of a single-vortex state at the KT phase transition of the 2D *XY* model, in comparison with that of a spin-wave state. The dynamic effect of the topological defect will be emphasized. We demonstrate that it is essential to introduce a local pseudo-magnetization to characterize the symmetric structure of the dynamic systems, which is defined as the projection of the spin configuration onto the metastable state or low-energy excited state. In section 2 the model and scaling analysis are described, and in section 3 the numerical results are presented. In section 4, theoretical calculations based on the linearized long-wave approximation are presented. Section 5 includes the conclusions.

2. Model and scaling analysis

2.1. Model

The 2D *XY* model is the simplest model for magnetic materials, exhibiting a KT phase transition. The Hamiltonian is written as

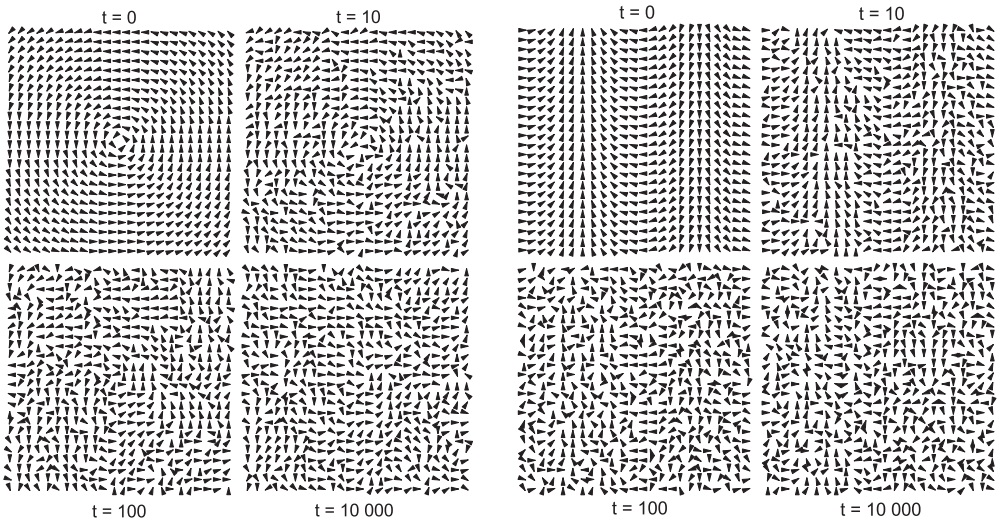

Figure 1. Dynamic relaxation of a vortex state and a spin-wave state is displayed, respectively, in (*a*) and (*b*), for the 2D *XY* model at the temperature $T = 0.89$, slightly below T_{KT}. The arrowhead denotes the orientation of the spin.

$$-\frac{1}{kT}H = K\sum_{\langle ij\rangle}\vec{S}_i\cdot\vec{S}_j, \tag{1}$$

where $\vec{S}_i = (S_{i,x}, S_{i,y})$ is a planar unit vector at site i of a square lattice, the sum is over the nearest neighbors and T is the temperature. In our notation, we simply take $K = 1/T$. In the literatures, the transition temperature T_{KT} is reported to be between 0.89 and 0.90 for the 2D *XY* model [43–45]. Below T_{KT}, the system remains critical. To study the pure relaxation dynamics of model A, we adopt the 'heat-bath' algorithm of an one-spin flip, in which a trial move is accepted with probability $1/[1 + \exp(\Delta E/T)]$, where ΔE is the energy change associated with the move.

To study the dynamic relaxation of a single-vortex state, we first construct a *perfect* vortex as the initial state. We put the vortex on a square lattice $L \times L$, and choose the center of the vortex as the origin of the polar coordinates. To reduce the finite-size effect, we apply antisymmetric boundary conditions with respect to the origin, i.e. $\vec{S}_{\vec{r}} = -\vec{S}_{-\vec{r}}$, which mimic the vortex line on the boundary. In figure 1(*a*), the dynamic evolution of the spin configuration is illustrated. Due to the vortex initial state, the dynamic system is *inhomogeneous* for different radius r. After the statistical average, the orientations of the spins form circular vortex lines. Except for the topological defect at the center, the vortex state is locally ordered, although globally it is still different from an ordered state. Naively, we may measure the magnetization along the circular vortex lines as a function of r and t. From the symmetry of the initial state, however, both the x and y components of the magnetization are zero.

In order to characterize the dynamic relaxation of the vortex state, therefore, we should introduce a *local pseudo-magnetization* and its second moment by the projection to the metastable state,

$$M_p^{(k)}(t,r) = \frac{1}{N_r^k}\left\langle\left[\sum_{\varphi=1}^{N_r}\vec{S}_{r\varphi}(t)\cdot\vec{S}_{r\varphi,p}\right]^k\right\rangle, \quad k=1,2; \tag{2}$$

$$M_n^{(k)}(t,r) = \frac{1}{N_r^k}\left\langle\left[\sum_{\varphi=1}^{N_r}\vec{S}_{r\varphi}(t)\cdot\vec{S}_{r\varphi,n}\right]^k\right\rangle, \quad k=1,2, \tag{3}$$

where $\langle\cdots\rangle$ represents the statistical average, and $N_r \approx 2\pi r$ is the number of the lattice sites at radius r. In the case now, the metastable state is just the perfect vortex, the same as the initial state, $\vec{S}_{r\varphi,p} = \vec{S}_{r\varphi}(0) = \vec{e}_\varphi$, while $\vec{S}_{r\varphi,n} = \vec{e}_r$ denotes the unit vector *perpendicular* to $\vec{S}_{r\varphi,p}$, i.e. that of the normal direction. In other words, $M_p^{(k)}(t,r)$ is the kth moment of the tangent direction, and $M_n^{(k)}(t,r)$ is that of the normal direction. From the symmetry of the vortex initial state, the normal component of the pseudo-magnetization is zero, i.e. $M_n(t,r) = 0$. Denoting $M(t,r) \equiv M_p(t,r)$ and $M^{(2)}(t,r) \equiv M_p^{(2)}(t,r) + M_n^{(2)}(t,r)$, we then define a time-dependent Binder cumulant,

$$U(t,r) = \frac{M^{(2)}(t,r)}{M(t,r)^2} - 1. \tag{4}$$

The Binder cumulant $U(t,r)$ describes the fluctuation of the pseudo-magnetization.

To investigate the dynamic effect of quenched disorder, we may randomly fix the orientations of the four spins at the center of the vortex during the dynamic evolution. Such a dynamic system is topologically similar to the dynamic relaxation around a disordered surface [21, 31]. Experimentally, a vortex state may be prepared by applying an electric current perpendicular to the lattice plane.

For comparison, we now consider the dynamic relaxation starting from a low-energy excited state, i.e. a spin-wave state. The spin wave is linearly polarized in the x direction, while ordered in the y direction. The simulation is performed with a rectangle lattice $L_x \times L_y$. In figure 1(b), the dynamic evolution of the spin configuration is displayed. The spin-wave state is locally ordered, but globally not. For such a dynamic process, we may naively measure the *line* magnetization along the x direction as a function of t. Obviously, the magnetization is zero due to the periodicity of the spin-wave state.

In order to characterize the dynamic relaxation starting from the spin-wave state, we may also define a pseudo-magnetization and its second moment as functions of t,

$$M_p^{(k)}(t) = \frac{1}{L_x^k}\left\langle\left[\sum_{x=1}^{L_x}\vec{S}_{xy}(t)\cdot\vec{S}_{xy,p}\right]^k\right\rangle, \qquad k=1,2; \tag{5}$$

$$M_n^{(k)}(t) = \frac{1}{L_x^k}\left\langle\left[\sum_{x=1}^{L_x}\vec{S}_{xy}(t)\cdot\vec{S}_{xy,n}\right]^k\right\rangle, \qquad k=1,2, \tag{6}$$

where $\vec{S}_{xy,p} = \vec{S}_{xy}(0)$, $\vec{S}_{xy,n}$ denotes the unit vector perpendicular to $\vec{S}_{xy,p}$, and $\langle\cdots\rangle$ represents both the statistical average and the average in the y direction. As shown in figure 1(b), $\vec{S}_{xy}(0)$ periodically changes its orientation along the x direction, but independent of y. From the periodicity of the spin-wave state, $M_n(t) = 0$. Denoting $M(t) \equiv M_p(t)$ and $M^{(2)}(t) \equiv M_p^{(2)}(t) + M_n^{(2)}(t)$, we then define a time-dependent Binder cumulant,

$$U(t) = \frac{M^{(2)}(t)}{M(t)^2} - 1. \tag{7}$$

2.2. Scaling analysis

In the critical regime, there are three spatial length scales in the dynamic relaxation of the vortex state, i.e. the nonequilibrium spatial correlation $\xi(t)$, the radius r of the circular vortex line and the lattice size L. Therefore, general scaling arguments lead to the scaling forms of the magnetization and its second moment,

$$M^{(k)}(t, r, L) = \xi(t)^{-k\eta/2}\widetilde{M}^{(k)}(r/\xi(t), \xi(t)/L), \qquad k = 1, 2, \tag{8}$$

where η is the static exponent. In the equation, the factor $\xi(t)^{-k\eta/2}$ indicates the scaling dimension of $M^{(k)}$ and the scaling function $\widetilde{M}^{(k)}(r/\xi(t), \xi(t)/L)$ represents the scale invariance of the dynamic system. In general, we expect that the scaling forms in equation (8) hold already in the *macroscopic* short-time regime, after a microscopic timescale $t_{\rm mic}$ [1, 3]. Our numerical simulations show, however, that only the pseudo-magnetization and its second moment obey such scaling forms.

In the short-time regime, i.e. the regime with $\xi(t) \ll L$, the pseudo-magnetization is independent of L. Then, the scaling form is simplified to

$$M(t, r) = \xi(t)^{-\eta/2}\widetilde{M}(r/\xi(t)). \tag{9}$$

Since the spatially correlating terms in the susceptibility $M^{(2)}(t, r) - M(t, r)^2$ can be neglected for $\xi(t) \ll r$, one may deduce $U(t, r) \sim 1/N_r^{d-1}$ for large r, with $d = 2$. Here, $N_r \propto r$ is the number of the lattice sites at radius r, similar to the lattice size L in [3, 21, 22]. Furthermore, $U(t, r)$ is independent of the scaling variable $\xi(t)/L$ in the short-time regime. Together with equations (8) and (9), one may write down the scaling form

$$U(t, r) = [\xi(t)/r]^{d-1}\widetilde{U}(r/\xi(t)). \tag{10}$$

The Binder cumulant is interesting; for the static exponent η is *not* involved.

For the critical dynamics of a continuous phase transition, $\xi(t)$ usually grows by a power law $\xi(t) \sim t^{1/z}$ and z is the so-called dynamic exponent. In shorter times, there may be corrections to scaling, typically in a power-law form

$$\xi(t) \sim t^{1/z}(1 + c/t^b). \tag{11}$$

For magnetic systems with a KT phase transition, e.g., the 2D *XY* model, the correction to scaling is weak in the dynamic relaxation with an *ordered* initial state, the dynamic exponent is theoretically expected to be $z = 2$ and numerical simulations indicate $b \approx 1$ [6, 19]. Due to the dynamic effect of the vortex-pair creation and annihilation, however, the correction to scaling becomes strong in the dynamic relaxation with a *disordered* initial state, and both theoretical and numerical calculations lead to a logarithmic form [37, 46, 6, 47, 19]

$$\xi(t) \sim [t/(lnt + c)]^{1/z}. \tag{12}$$

Theoretically, equation (12) is equivalent to equation (11) in the limit $b \to 0$. Numerically detecting a logarithmic correction to scaling is rather notorious, for it is negligible only in the limit $t \to \infty$ [6, 47, 19]. Recently, a logarithmic correction to scaling is detected inside the domain interface, which is also attributed to the vortex-pair creation and annihilation [22].

In this paper, we will show that there exists a *core* of the vortex state and there emerges a strong logarithmic correction to scaling in the core, again due to the vortex-pair creation and annihilation. The core of the vortex grows with time and also roughens. Such a phenomenon is rather similar to the propagation and roughening of the domain interface [21–23]. Outside the core of the vortex and also for the spin-wave initial state, the dynamic system is locally ordered. Therefore, the dynamic relaxation is similar to that with the ordered initial state, and the correction to scaling is in a weak power-law form. Furthermore, we demonstrate that

a limited amount of quenched disorder in the core of the vortex may change the dynamic universality class, i.e. the scaling functions $\widetilde{M}^{(k)}(s)$ in equation (8) and the corresponding critical exponents.

For the dynamic relaxation with the spin-wave initial state, there are two spatial length scales in the dynamic system, i.e. the nonequilibrium spatial correlation $\xi(t)$ and the lattice size L_x, if the lattice size L_y is sufficiently large. Therefore, scaling arguments lead to the scaling form of the pseudo-magnetization and its second moment,

$$M^{(k)}(t, L_x) = \xi(t)^{-k\eta/2}\widetilde{M}^{(k)}(\xi(t)/L_x), \qquad k = 1, 2. \tag{13}$$

For the pseudo-magnetization, the scaling function $\widetilde{M}(\xi(t)/L_x)$ is independent of L_x in the thermodynamic limit $L_x \to \infty$. The scaling form is simplified to

$$M(t) \sim \xi(t)^{-\eta/2}. \tag{14}$$

The scaling behavior of the Binder cumulant is

$$U(t) \sim [\xi(t)/L_x]^{d-1}. \tag{15}$$

3. Monte Carlo simulation

For the dynamic relaxation with the vortex initial state, our main results are obtained with $L = 256$ at $T_{\mathrm{KT}} = 0.89$, and the maximum updating time is $t_M = 10\,240$ Monte Carlo time steps. A Monte Carlo time step is defined by a sweep over all spins on the lattice. Additional simulations with $L = 128$ and 512 are performed to investigate the finite-size scaling behavior and finite-size effect. Total samples for the average are about 20 000. For the dynamic relaxation with the spin-wave initial state, the main results are obtained with $L_x \times L_y = 256 \times 256$ and $L_x \times L_y = 512 \times 256$ at $T_{\mathrm{KT}} = 0.89$, and the maximum updating time is $t_M = 10\,240$ Monte Carlo time steps. Additional simulations with $L_x \times L_y = 128 \times 256$ and $L_x \times L_y = 1024 \times 256$ are also performed. Total samples for average are about 10 000. Statistical errors are estimated by dividing the total samples into two or three subgroups. If the fluctuation in the time direction is comparable with or larger than the statistical error, it will be taken into account. Theoretically, the scaling forms described in the previous section hold in the macroscopic short-time regime, after a microscopic timescale t_{mic}. t_{mic} is not universal and relies on microscopic details of the dynamic systems. In our simulations, t_{mic} is about 100 Monte Carlo time steps.

3.1. Vortex state

For the dynamic relaxation with the vortex initial state, the time evolution of the local pseudo-magnetization $M(t, r) \equiv M_p^{(1)}(t, r)$ defined in equation (2) is displayed in figure 2(*a*). Monte Carlo simulations have been performed with the lattice sizes $L = 256$ and 512, and the finite-size effect is negligibly small. Denoting $s = r/\xi(t)$, we observe that for a sufficiently large s, e.g., $r = 127.5$ and $t < t_M = 10\,240$, $M(t, r)$ approaches the power-law decay *at bulk*, i.e. $M(t, r) \sim t^{-\eta/2z}$, while for a sufficiently small s, e.g., $r = 0.707$ and $t > 100$, $M(t, r)$ also exhibits a power-law behavior, but decays *much faster* than at bulk. In other words, the scaling function $\widetilde{M}(s)$ in equation (9) is characterized by

$$\widetilde{M}(s) \sim \begin{cases} \text{const} & s \to \infty \\ s^{\eta_0/2} & s \to 0. \end{cases} \tag{16}$$

Here, η_0 is the vortex exponent. We call the regime with small s the *core* of the vortex state. The spatial length scale of the core increases with time, and it is just proportional to

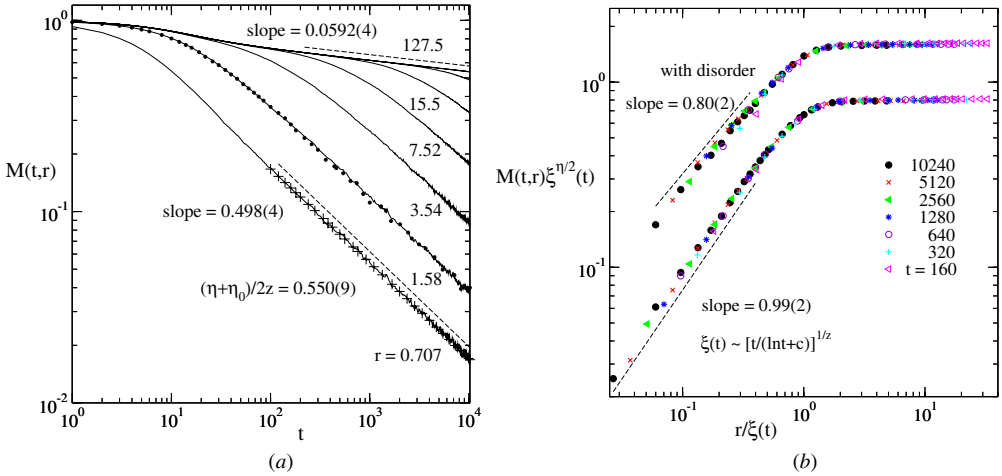

Figure 2. (*a*) The time evolution of the pseudo-magnetization of the 2D *XY* model starting from the vortex state is displayed for different radius r on a double-log scale. Simulations are performed with $L = 256$, and solid dots are the data obtained with $L = 512$. Dashed lines represent power-law fits, and pluses indicate the fit with a logarithmic correction to scaling. (*b*) The scaling function $\widetilde{M}(r/\xi(t)) = M(t, r)\xi(t)^{\eta/2}$ is plotted on a double-log scale. In the core of the vortex, the logarithmic correction to scaling is taken into account, and $c = 5.45$ is from the fitting in (*a*). Data collapse is observed for different t. The dashed line shows a power-law fit.

the nonequilibrium correlation length $\xi(t)$. Outside the core of the vortex, i.e. the regime with large s, the dynamic relaxation of the pseudo-magnetization is governed by the bulk exponent η, while in the core of the vortex, it is controlled by both the bulk exponent η and the vortex exponent η_0. Outside the core of the vortex, the dynamic relaxation of the pseudo-magnetization is the same as that with an ordered initial state, and the correction to scaling is weak. Assuming $\xi(t) \sim t^{1/z}$, one deduces $M(t, r) \sim t^{-\eta/2z}$ for $s \to \infty$. In figure 2(*a*), the exponent $\eta/2z = 0.0592(4)$ measured from the slope of the curve of $r = 127.5$ is in agreement with that for the ordered initial state [6, 22], and it is also consistent with $\eta = 0.234(2)$ and $z = 2$ reported in the literatures [6]. A power-law correction to scaling slightly refines the result by about 1%, and yields $\eta/2z = 0.0586$. In fact, the exponent η extracted in most of the numerical simulations is somewhat smaller than the prediction of the KT theory, $\eta = 1/4$. This might imply that the KT theory is not exact for the *XY* model [43]. In the core of the vortex, one may similarly derive $M(t, r) \sim t^{-(\eta+\eta_0)/2z}$ for $s \to 0$. Then, one measures $(\eta + \eta_0)/2z = 0.498(4)$ from the slope of the curve of $r = 0.707$ and calculates $\eta_0/2 = 0.878(8)$ by taking $z = 2$ as input.

For the domain interface of the 2D *XY* model, the interface exponent $\eta_0/2$ is reported to be 0.997(7), very close to 1 [22]. It indicates that $M(t, r)$ is an analytic function of r. Topologically, a vortex state could be transformed from either a domain interface or a free surface. Physically, the former seems closer to a vortex state. Is the vortex exponent $\eta_0/2$ really different from 1? According to the scaling form in equation (16), the r-dependence and t-dependence of the magnetization $M(t, r)$ should yield a same exponent $\eta_0/2$. We observe that at a fixed time t, the r-dependence of $M(t, r)$ is very close to linear in the small r regime. According to equation (16), this indicates $\eta_0/2 \approx 1$, contracting to $\eta_0/2 = 0.878(8)$ from the power-law fit in figure 2(*a*). Our thought is that there exists a strong logarithmic correction in the growth law of $\xi(t)$, described by equation (12). Such a fitting to the curve of $r = 0.707$ in figure 2(*a*) yields $(\eta + \eta_0)/2z = 0.550(9)$. With $\eta/2z = 0.0586$ as input, one then calculates the vortex exponent $\eta_0/2 = 0.983(18)$, also close to 1. To further confirm this result, let us

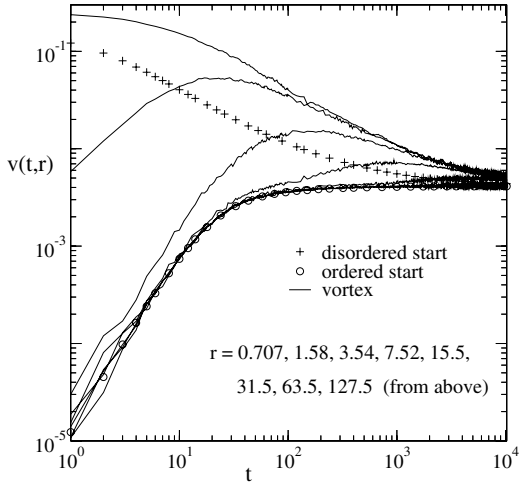

Figure 3. The time evolution of the vortex density in the dynamic relaxation of a vortex state in comparison with that in the dynamic relaxation starting from ordered and disordered states.

fully examine the scaling form in equations (9) and (16). In figure 2(*b*), the scaling function $\widetilde{M}(r/\xi(t)) = M(t, r)\xi(t)^{\eta/2}$ is plotted, and data collapse is clearly observed for different time t. In the small-s regime, the logarithmic correction to scaling described by equation (12) has been taken into account, and the constant $c = 5.45$ is taken from the fitting in figure 2(*a*). Obviously, $\widetilde{M}(s)$ exhibits a power-law behavior in the small-s regime, supporting the linear r-dependence of $M(t, r)$. From the slope of the curve of $t = 10\,240$, one measures $\eta_0/2 = 0.99(2)$, rather close to 1, and consistent with $\eta_0/2 = 0.983(18)$ obtained from figure 2(*a*). For large s, $\widetilde{M}(s)$ approaches a constant. Finally, we mention that in the data collapse in figure 2(*b*), data points for all r including $r = 0.707$ are plotted, although those for $t \leqslant t_{\rm mic} \sim 100$ or 200 are truncated. In other words, the dynamic scaling behavior holds even in the very center of the vortex state.

The logarithmic correction to scaling at the KT phase transition is believed to be induced by the vortex-pair creation and annihilation. Therefore, we measure the time evolution of the vortex density for different r, in comparison with those in the dynamic relaxation starting from ordered and disordered states. The vortex density is defined as

$$v(t, r) = \langle |v_p| \rangle, \qquad v_p = \sum_{p(r,\varphi)} [\theta_i(t) - \theta_j(t)]/2\pi, \tag{17}$$

where θ_i and θ_j denote the orientational angles of $\vec{S}_i$ and $\vec{S}_j$, $(\theta_i - \theta_j)$ are valued within the interval $[-\pi, \pi]$, the sum is over the four links (i, j) of the clockwise plaquette at site (r, φ) and $\langle \cdots \rangle$ represents both the statistical average and the average in the φ direction. Numerical results are shown in figure 3. Outside the core of the vortex, e.g., at $r = 127.5$, the vortex density is initially zero, then increases with time and finally reaches the steady value in equilibrium. This dynamic process is relatively fast, the same as that in the dynamic relaxation with the ordered initial state. In the core of the vortex, e.g., at $r = 0.707$ or 1.58, the vortex density initially increases rapidly to a large value, which even exceeds that of the disordered initial state, then decreases slowly and finally relaxes to the equilibrium. This dynamic process is even slower than that with the disordered initial state. Therefore, it is not surprising that a strong logarithmic correction to scaling emerges.

Here, we should emphasize that the slow dynamic relaxation in the core of the vortex state is indeed induced by the topological structure. For example, we may simulate the dynamic

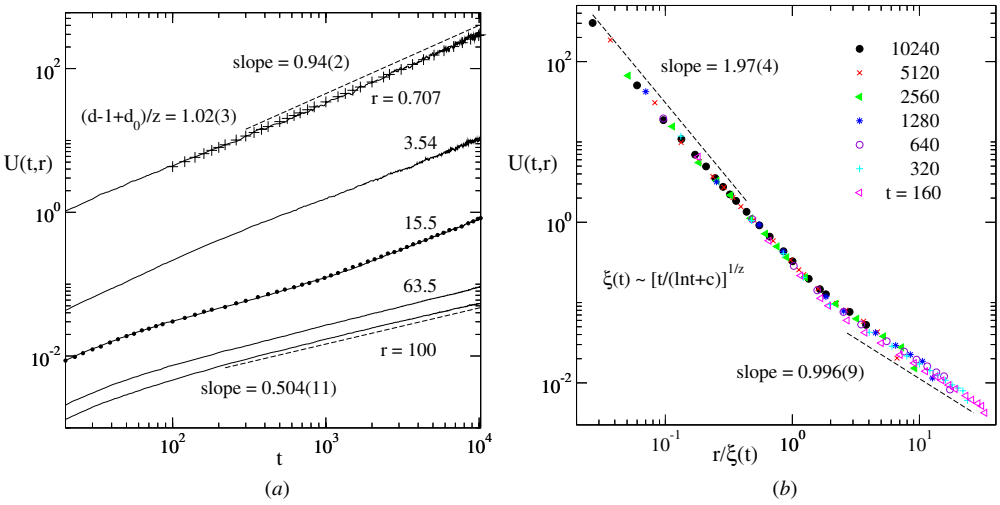

Figure 4. (*a*) The time evolution of the Binder cumulant of the 2D *XY* model starting from the vortex state is displayed for different radius r on a double-log scale. Simulations are performed with $L = 256$, and solid dots are the data obtained with $L = 512$. Dashed lines represent power-law fits, and pluses indicate the fit with a logarithmic correction to scaling. (*b*) Data collapse of the Binder cumulant is displayed for different t. In the core of the vortex, the logarithmic correction to scaling is taken into account, and $c = 5.45$. Dashed lines show power-law fits.

relaxation for the initial state with a four-spin vortex on the ordered or disordered background. The pseudo-magnetization rapidly drops to zero.

To clarify the scaling form of the Binder cumulant for the dynamic relaxation of a vortex state, we plot $U(t, r)$ as a function of t for different radius r in figure 4(*a*). Similar to equation (16), we expect the scaling function $\widetilde{U}(s)$ in equation (10) to be

$$\widetilde{U}(s) \sim \begin{cases} \text{const} & s \to \infty \\ s^{-d_0} & s \to 0. \end{cases} \tag{18}$$

In the core of the vortex state, e.g., $r = 0.707$, $U(t, r)$ looks like exhibiting a power-law behavior, and the slope of the curve is 0.94(2). Assuming $\xi(t) \sim t^{1/z}$, one derives $U(t) \sim t^{(d-1+d_0)/z}$. From $(d - 1 + d_0)/z = 0.94(2)$, one calculates $d_0 = 0.88(4)$. With the logarithmic correction in equation (12), however, the fitting yields $d_0 = 1.04(6)$, close to 1. To further confirm this result, we may fully examine the scaling form in equations (10) and (18). In figure 4(*b*), $U(t, r)$ is plotted as a function of $s = r/\xi(t)$. Data collapse is observed for different time t. In the core of the vortex, the logarithmic correction to scaling has been taken into account. Obviously, $U(t, r)$ exhibits a power-law behavior in the core of the vortex. From the slope of the curves, one measures $d-1+d_0 = 1.97(4)$, then calculates $d_0 = 0.97(4)$, and it supports that d_0 is close to 1. For comparison, the exponent d_0 for the domain interface is close to 2 [22]. The reason is that the domain interface is a one-dimensional object, while the core of the vortex is effectively zero dimensional. It is interesting that the pseudo-magnetization of the zero-dimensional vortex core exhibits a similar dynamic behavior as that of the one-dimensional domain interface, but its fluctuation is different. In fact, the fluctuation of the pseudo-magnetization at the core of the vortex state does not show r-dependence. Therefore, we have the simple relation $d_0 = \eta_0 - (d - 1)$.

Outside the core of the vortex, e.g., $r = 100$, a power-law behavior is observed in figure 4(*a*), and the slope of the curve is 0.504(11). Assuming $\xi(t) \sim t^{1/z}$, one derives $U(t, r) \sim t^{(d-1)/z}$. From $(d - 1)/z = 0.504(11)$, we obtain $z = 1.98(4)$, consistent

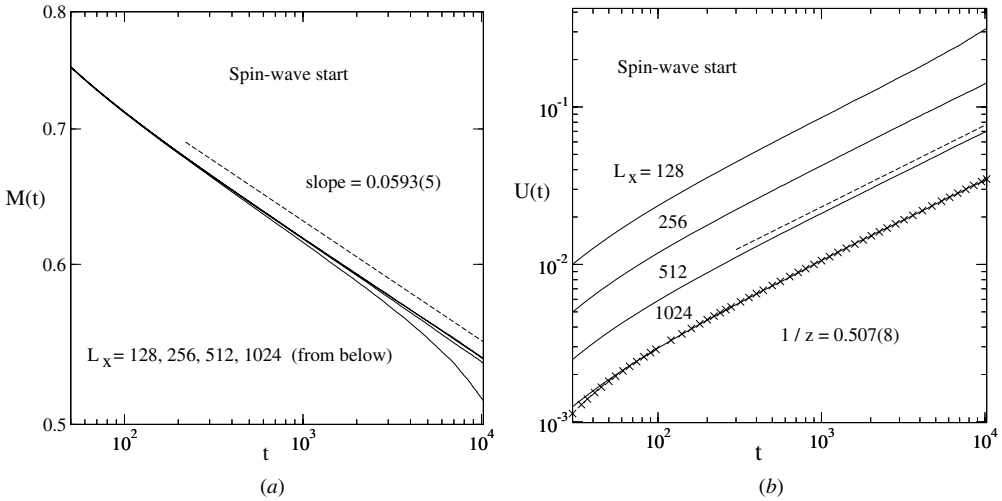

Figure 5. In (*a*) and (*b*), the pseudo-magnetization and the Binder cumulant of the 2D *XY* model starting from the spin-wave state are plotted on a double-log scale. Dashed lines show power-law fits, while crosses indicate the fitting with a power-law correction to scaling.

with the theoretical value $z = 2$. At the same time, we may also examine the behavior $U(t, r) \sim s^{-(d-1)}$ in the large-s regime in figure 4(*b*). From the slope of the curves, one measures $d - 1 = 0.996(9)$. Since the maximum radius of the vortex line is $r = L/2$ in the square lattice, the dynamic behavior of the Binder cumulant becomes unreasonable for $r \geqslant L/2$. Due to this boundary effect, the data collapse of the Binder cumulant in figure 4(*b*) is less good for large s, compared with that for small s and for the magnetization shown in figure 2(*b*).

3.2. Vortex state with quenched disorder

To study the dynamic effect of quenched disorder and to further demonstrate the importance of the topological structure of the vortex state, we randomly fix the orientations of the four spins at the center of the vortex and repeat the simulation of the dynamic relaxation of the vortex state and analysis of the pseudo-magnetization according to equations (9) and (16). The scaling function $\widetilde{M}(r/\xi(t))$ is plotted in figure 2(*b*), and data collapse is also observed. However, the vortex exponent is modified to $\eta_0/2 = 0.80(2)$, significantly different from $\eta_0/2 = 0.99(2)$ for the case without disorder. Such a scenario is similar to the dynamic relaxation around a disordered surface [21, 31]. But here disorder exists only at four lattice sites in the core of the vortex state.

Topologically, the vortex state may be compared with a DW or a surface. It is interesting that the dynamic relaxation of the vortex state is similar to that of a DW rather than a surface, i.e. $\eta_0/2 = 1.0$. However, a limited amount of quenched disorder around the center of the vortex could modify the dynamic universality class, leading to $\eta_0/2 = 0.80(2)$. This again shows that the topological structure of the vortex state is crucial.

3.3. Spin-wave state

For the spin-wave initial state, the time evolution of the pseudo-magnetization is displayed in figure 5(*a*). Since the spin-wave state is locally ordered, the dynamic relaxation of the pseudo-magnetization is expected to be similar to that with the ordered initial state, $M(t) \sim t^{-\eta/2z}$, *without* an logarithmic correction to scaling. In fact, if one computes the vortex density $v(t)$,

it completely overlaps with that of the dynamic relaxation starting from an ordered state as shown in figure 3. In figure 5(*a*), the exponent $\eta/2z = 0.0593(5)$ is estimated from the slope of the curve of $L_x = 512$ and 1024. A power-law correction to scaling refines the measurement to $\eta/2z = 0.0586(3)$, with $b = 1$ and $c = -11.1$.

For the dynamic relaxation with both the vortex and spin-wave initial states, the standard magnetization is zero from the beginning of the time evolution. Only the local pseudo-magnetization could characterize the dynamic systems.

For the spin-wave initial state, the time evolution of the Binder cumulant is displayed in figure 5(*b*). The dynamic relaxation of the Binder cumulant is similar to that with an ordered initial state. Assuming $\xi(t) \sim t^{1/z}$, one deduces $U(t) \sim t^{(d-1)/z}$. In figure 5(*b*), the slope of the curves of $L_x = 512$ and 1024 is estimated to be 0.520(3). Obviously, there exists a correction to scaling in the growth law of $\xi(t)$, and the fitting with equation (11) yields an exponent $(d-1)/z = 0.507(8)$, consistent with the theoretical value $z = 2$. Finally, the finite-size dependence $U(t) \sim 1/L_x^{d-1}$ can also be verified with the data in figure 5(*b*).

4. Theoretical calculation

Based on the linearized long-wave approximation, we may theoretically derive the scaling forms for the dynamic relaxation with the spin-wave and vortex initial state. Here, we just report the main results and leave the detailed calculations in the appendix. For the spin-wave initial state, the local pseudo-magnetization is independent of $\vec{R}$,

$$M_p(t, \vec{R}) \propto t^{-\eta/2z}. \tag{19}$$

This power-law behavior is in agreement with the scaling form in equation (14). For the vortex initial state, the scaling form of the pseudo-magnetization is

$$M_p(t, r') = t^{-\eta/2z} \sin\left(\sqrt{\pi} \int_0^{r'} \mathrm{d}R' \, \mathrm{e}^{-R'^2}\right), \tag{20}$$

where $r' = r/\sqrt{4a^2 t/T} \propto r/t^{1/z} = s$. This result is principally in agreement with the scaling forms in equations (9) and (16), although the logarithmic correction is still absent due to the linearized long-wave approximation in equation (A.1). For small r', $M_p(t, r') \sim t^{-\eta/2z} s$; therefore, $\eta_0/2 = 1$.

5. Conclusion

With Monte Carlo methods, we have simulated the dynamic relaxation starting from both a vortex state and a spin-wave state at the KT phase transition of the 2D *XY* model. The dynamic scaling behavior of the local pseudo-magnetization and Binder cumulant is carefully analyzed. Taking into account the logarithmic correction, the vortex exponent $\eta_0/2 = 0.99(2)$ is extracted. A limited amount of quenched disorder in the center of the vortex alters the dynamic universality class, and the vortex exponent is estimated to be $\eta_0/2 = 0.80(2)$. In table 1, all measurements of the critical exponents are summarized, compared with those in the literatures. Finally, theoretical calculations based on the linearized long-wave approximation are presented, and the scaling forms for the dynamic relaxation with the spin-wave and vortex initial states are derived.

Our numerical and theoretical results show that the local pseudo-magnetization is a useful concept in characterizing the relaxation dynamics starting from a metastable state or a low-energy excited state. Further applications of the methodology to complex dynamic systems such as spin glasses are interesting.

Table 1. Critical exponents estimated from the relaxation dynamics of the vortex state and spin-wave state, in comparison with those from the DW dynamics and STD. In the last column, quenched disorder is located at the vortex center.

	STD [6]	DW [22]	Spin wave	Vortex	Disorder
η	0.234(2)	0.234(2)	0.234(2)	0.234(2)	
$\eta_0/2$		1.00(1)		0.99(2)	0.80(2)
d_0		1.99(1)		0.97(4)	0.78(3)
z	2.01(1)	1.99(4)	1.97(4)	1.98(4)	

Acknowledgment

This work was supported in part by NNSF of China under grant nos 10875102 and 11075137.

Appendix. Theoretical calculation

In this appendix, we theoretically derive the scaling forms for the dynamic relaxation with the spin-wave initial state and the vortex initial state, based on the linearized long-wave approximation. In the Hamiltonian in equation (1), the spin $\vec{S}_i$ can be represented by an angle, i.e. $\vec{S}_i = (\cos\theta_i, \sin\theta_i)$. With the linearized long-wave approximation, the Hamiltonian can be reduced,

$$\begin{aligned} H &= -\sum_{\langle ij\rangle}\cos(\theta_i-\theta_j) \approx \frac{1}{2}\sum_{\langle ij\rangle}(\theta_i-\theta_j)^2 + H_0 \\ &= \frac{1}{4}\sum_{\vec{R},\vec{a}}(\theta(\vec{R})-\theta(\vec{R}+\vec{a}))^2 + H_0, \end{aligned} \tag{A.1}$$

where $\vec{R}$ is the position vector of a lattice site and $\vec{a}$ is the spacing vector between the site and its nearest neighbors. The constant H_0 will be ignored in the following calculations. After the Fourier transformation, the Hamiltonian is rewritten as

$$H = \frac{1}{2}\sum_{\vec{k}} J(\vec{k})|\theta(\vec{k})|^2. \tag{A.2}$$

Here, $J(\vec{k})$ can be simplified with the long-wave approximation,

$$J(\vec{k}) = \frac{1}{2}\sum_{\vec{a}}|1-\mathrm{e}^{\mathrm{i}\vec{k}\cdot\vec{a}}|^2 \approx a^2k^2. \tag{A.3}$$

The relaxation dynamics of model A for the *XY* model can be described by the Langevin equation

$$\frac{\mathrm{d}\theta(t,\vec{k})}{\mathrm{d}t} = -\frac{1}{T}\frac{\partial H}{\partial\theta(t,\vec{k})} + \epsilon(t,\vec{k}) = -\frac{a^2k^2}{T}\theta(t,\vec{k}) + \epsilon(t,\vec{k}), \tag{A.4}$$

$$\theta(t,\vec{k}) = \frac{a}{2\pi}\int \mathrm{d}R\,\mathrm{e}^{-\mathrm{i}\vec{k}\cdot\vec{R}}\theta(t,\vec{R}). \tag{A.5}$$

Here, $\epsilon(t,\vec{k})$ is a Gaussian white noise with $\langle\epsilon(t,\vec{k})\epsilon(t',\vec{k}')\rangle = 2\delta(\vec{k}+\vec{k}')\delta(t-t')$, and $\langle\cdots\rangle$ represents the statistical average. Since the equation is linear, it can be exactly solved,

$$\theta(t,\vec{k}) = \int_0^t \mathrm{e}^{-a^2k^2(t-t')/T}\epsilon(t',\vec{k})\,\mathrm{d}t' + \theta(0,\vec{k})\,\mathrm{e}^{-a^2k^2t/T}. \tag{A.6}$$

One may easily calculate $\langle\theta(t,\vec{k})\rangle = \theta(0,\vec{k})\,\mathrm{e}^{-a^2k^2t/T}$ and

$$\langle|\theta(t,\vec{k})|^2\rangle = \frac{T}{a^2k^2}(1-\mathrm{e}^{-2a^2k^2t/T}) + |\theta(0,\vec{k})|^2\,\mathrm{e}^{-2a^2k^2t/T}. \tag{A.7}$$

In equation (A.6), $\theta(t,\vec{k})$ consists of two parts, the bulk one $F(t,\vec{k})$ and the initial-condition-dependent one $G(t,\vec{k})$,

$$F(t,\vec{k}) = \int_0^t \mathrm{e}^{-a^2k^2(t-t')/T}\epsilon(t',\vec{k})\,\mathrm{d}t', \qquad G(t,\vec{k}) = \theta(0,\vec{k})\,\mathrm{e}^{-a^2k^2t/T}. \tag{A.8}$$

From the inverse Fourier transformation, one calculates $F(t,\vec{R})$ and $G(t,\vec{R})$ and then obtains the complex magnetization,

$$M_x(t,\vec{R}) + \mathrm{i}M_y(t,\vec{R}) = \langle\mathrm{e}^{\mathrm{i}\theta(t,\vec{R})}\rangle = \langle\mathrm{e}^{\mathrm{i}F(t,\vec{R})}\rangle\,\mathrm{e}^{\mathrm{i}G(t,\vec{R})}. \tag{A.9}$$

Using the cumulant expansion and the result $\langle F(t,\vec{R})\rangle = 0$, one deduces

$$\begin{aligned} M_x(t,\vec{R}) &= \mathrm{e}^{-\langle F^2(t,\vec{R})\rangle/2}\cos(G(t,\vec{R})),\\ M_y(t,\vec{R}) &= \mathrm{e}^{-\langle F^2(t,\vec{R})\rangle/2}\sin(G(t,\vec{R})). \end{aligned} \tag{A.10}$$

One may calculate

$$\begin{aligned} \langle F^2(t,\vec{R})\rangle &= \left(\frac{a}{2\pi}\right)^2\int \mathrm{d}\vec{k}\int \mathrm{d}\vec{k}'\langle F(t,\vec{k})F(t,\vec{k}')\rangle\,\mathrm{e}^{\mathrm{i}(\vec{k}+\vec{k}')\cdot\vec{R}}\\ &= \left(\frac{a}{2\pi}\right)^2\int \mathrm{d}\vec{k}\frac{T}{a^2k^2}(1-\mathrm{e}^{-2a^2k^2t/T})\\ &= \frac{T}{4\pi}\ln t + C, \end{aligned} \tag{A.11}$$

where C is an integral constant. Obviously the bulk part of $\theta(t,\vec{R})$ is independent of $\vec{R}$.

Now it is important to calculate the initial-condition-dependent part,

$$G(t,\vec{R}) = \frac{a}{2\pi}\int \mathrm{d}\vec{k}\,\mathrm{e}^{\mathrm{i}\vec{k}\cdot\vec{R}}G(t,\vec{k}). \tag{A.12}$$

For the ordered initial state, i.e. $\theta(0,\vec{R}) = \phi$, one calculates $G(t,\vec{R}) = \phi$ and

$$M_x(t,\vec{R}) \propto t^{-T/8\pi}\cos\phi,\, M_y(t,\vec{R}) \propto t^{-T/8\pi}\sin\phi. \tag{A.13}$$

Under the long-wave approximation, $\eta = T/2\pi$ and $z = 2$ [46]. Thus, the power-law behavior of the magnetization, i.e. $M \propto t^{-\eta/2z}$, agrees with that from the scaling theory and renormalization-group calculations [1, 3].

For the spin-wave initial state, i.e. $\theta(0,\vec{R}) = 2\phi\cos(k_0x)$ with $\vec{R} = (x,y)$,

$$G(t,x) = \frac{a}{2\pi}\int \mathrm{d}\vec{k}\,\mathrm{e}^{\mathrm{i}\vec{k}\cdot\vec{R}}G(t,\vec{k}) = 2\phi\cos(k_0x)\,\mathrm{e}^{-a^2k_0^2t/T}. \tag{A.14}$$

Since we only consider the case of small k_0, e.g., $k_0 \sim 1/L$, the time dependence in equation (A.14) can be ignored. Hence, $G(t,x)$ is approximately equal to $\theta(0,\vec{R})$. Then,

$$M_x(t,\vec{R}) \propto t^{-\eta/2z}\cos(2\phi\cos(k_0x)), \qquad M_y(t,\vec{R}) \propto t^{-\eta/2z}\sin(2\phi\cos(k_0x)). \tag{A.15}$$

Obviously the standard magnetization is zero. But the local pseudo-magnetization is non-zero. In fact the local pseudo-magnetization is independent of x,

$$M_p(t,\vec{R}) = \vec{M}(t,\vec{R})\cdot\vec{M}(0,\vec{R}) \propto t^{-\eta/2z}. \tag{A.16}$$

This power-law behavior is in agreement with the scaling form in equation (14).

How is the dynamic relaxation of a vortex state? In this case, $\theta(0,\vec{R}) = \varphi(\vec{R}) + \pi/2$, and $\varphi(\vec{R})$ is the polar angle of $\vec{R}$. According to equations (A.8) and (A.12), one can calculate

$$G(t,\vec{r}) = \frac{T}{4\pi t}\int \mathrm{d}\vec{R}\theta(0,\vec{R})\,\mathrm{e}^{-(\vec{R}-\vec{r})^2/(4a^2t/T)}. \tag{A.17}$$

Let us define $\vec{R'} = (\vec{R} - \vec{r})/\sqrt{4a^2t/T}$, $\vec{r'} = \vec{r}/\sqrt{4a^2t/T}$; then

$$G(t, \vec{r'}) = \frac{1}{\pi} \int \mathrm{d}R' R' \mathrm{e}^{-R'^2} \int \mathrm{d}\varphi(R') \theta(\vec{R'} + \vec{r'}, 0). \tag{A.18}$$

Due to the rotational symmetry, $G(t, \vec{r'}) - \theta(0, \vec{r'})$ is independent of $\varphi(\vec{r'})$. To simplify the calculations, we set $\vec{r'} = (r', 0)$, i.e. $\varphi(\vec{r'}) = 0$; thus,

$$\begin{aligned} G(t, \vec{r'}) - \theta(0, \vec{r'}) &= \frac{1}{\pi} \int \mathrm{d}R' R' \mathrm{e}^{-R'^2} \int \mathrm{d}\varphi(R') \varphi(\vec{R'} + \vec{r'}) \\ &= \frac{1}{\pi} \int_0^\infty \mathrm{d}R' R' \mathrm{e}^{-R'^2} \int_{-\pi}^{\pi} \mathrm{d}\varphi(R') \Theta(\varphi(R'), r'/R'), \end{aligned} \tag{A.19}$$

and $\Theta(\varphi(R'), r'/R')$ is introduced for convenience,

$$\Theta(\varphi(R'), r'/R') = \arctan\left[\cos\varphi(R') + \frac{r'}{R'}, \sin\varphi(R')\right]. \tag{A.20}$$

Here, $\arctan(x, y)$ is defined in the interval $[-\pi, \pi]$ by $\tan[\arctan(x, y)] = y/x$.

In fact, $\varphi(R')$ is the polar angle of $\vec{R'}$, and $\Theta(\varphi(R'), r'/R')$ is that of $\vec{R'} + \vec{r'}$. $\vec{r'}$ is the fixed site we are looking at, and $\vec{R'}$ is the site we should integrate. For $R' < r'$, $|\Theta(\varphi(R'), r'/R')| < \pi/2$ and $\Theta(\varphi(R'), r'/R')$ is a single-valued odd function of $\varphi(R')$. The integration over $\varphi(R')$ in equation (A.19) is zero. For $R' \geqslant r'$, $\Theta(\varphi(R'), r'/R')$ is still odd, but not single-valued at $\varphi(R') = \pm\pi$. When $\varphi(R') \to \pm\pi$, $\Theta(\varphi(R'), r'/R') \to \pm\pi$. However, $\varphi(R') = \pm\pi$ correspond to a same spatial point. Since $\Theta(\varphi(R'), r'/R')$ is multiple-valued at $\varphi(R') = \pm\pi$, the integration over $\varphi(R')$ in equation (A.19) can be non-zero.

From the above analysis, the integration in equation (A.19) can be rewritten as

$$G(t, \vec{r'}) - \theta(0, \vec{r'}) = \frac{1}{\pi} \int_{r'}^\infty \mathrm{d}R' R' \mathrm{e}^{-R'^2} \int_{-\pi}^{\pi} \mathrm{d}\varphi(R') \Theta(\varphi(R'), r'/R'). \tag{A.21}$$

Let us focus on the integration over $\varphi(R')$. Since $\Theta(\varphi(R'), r'/R')$ is an odd function, non-zero contribution only comes from a small interval around $\varphi(R') = \pm\pi$, and

$$\int_{-\pi}^{\pi} \mathrm{d}\varphi[\Theta(\varphi + \epsilon) - \Theta(\varphi - \epsilon)] = 2 \int_{-\pi}^{\pi} \mathrm{d}\varphi \Theta(\varphi), \tag{A.22}$$

where ϵ is a small angle to be determined. Substituting equation (A.22) into equation (A.21),

$$\begin{aligned} G(t, \vec{r'}) - \theta(0, \vec{r'}) &= \frac{1}{2\pi} \int_{r'}^\infty \mathrm{d}R' R' \, \mathrm{e}^{-R'^2} \int_{-\pi}^{\pi} \mathrm{d}\varphi[\Theta(\varphi + \epsilon) - \Theta(\varphi - \epsilon)] \\ &= \frac{1}{2\pi} \int_{r'}^\infty \mathrm{d}R' R' \, \mathrm{e}^{-R'^2} \int_{-\pi}^{\pi} \mathrm{d}\Theta \frac{\Delta}{R'} \\ &= \pm \Delta \int_{r'}^\infty \mathrm{d}R' \, \mathrm{e}^{-R'^2}. \end{aligned} \tag{A.23}$$

Here, $2\epsilon = \Delta/R'$ and $\oint \mathrm{d}\Theta = \pm 2\pi$ dependent on the existence of a vortex or anti-vortex.

The pseudo-magnetization can be calculated by $M_p(t, \vec{r'}) = t^{-\eta/2z} \cos(G(t, \vec{r'}) - \theta(0, \vec{r'}))$. When $r' \to \infty$, it approaches the bulk behavior $M_p(t, \vec{r'}) = t^{-\eta/2z}$. When $r' \to 0$, $M_p(t, \vec{r'}) = t^{-\eta/2z} \cos(\Delta\sqrt{\pi}/2)$. Due to the symmetry or from our numerical simulations, $M_p(t, 0)$ should be zero. Hence, the parameter $\Delta = \sqrt{\pi}$ is determined. The finial form of the pseudo-magnetization is then derived

$$M_p(t, r') = t^{-\eta/2z} \sin\left(\sqrt{\pi} \int_0^{r'} \mathrm{d}R' \, \mathrm{e}^{-R'^2}\right), \tag{A.24}$$

where $r' = r/\sqrt{4a^2t/T} \propto r/t^{1/z} = s$.

The linearized long-wave approximation in equation (A.1) is good for the dynamic relaxation of the spin-wave state, for the dynamic effect of the vortex-pair creation and annihilation is weak. For the dynamic relaxation of the vortex state, however, the linearized long-wave approximation could not catch the logarithmic correction in the core of the vortex. Additionally, a phenomenological technique has been used in the derivation of equations (A.23) and (A.24) to obtain the scaling form in the core of the vortex.

References

[1] Janssen H K, Schaub B and Schmittmann B 1989 *Z. Phys.* B **73** 539
[2] Huse D 1989 *Phys. Rev.* B **40** 304
[3] Zheng B 1998 *Int. J. Mod. Phys.* B **12** 1419 (review article)
[4] Zheng B, Schulz M and Trimper S 1999 *Phys. Rev. Lett.* **82** 1891
[5] Luo H J, Schülke L and Zheng B 1998 *Phys. Rev. Lett.* **81** 180
[6] Zheng B, Ren F and Ren H 2003 *Phys. Rev.* E **68** 046120
[7] Ozeki Y and Ito N 2003 *Phys. Rev.* B **68** 054414
[8] Granato E and Dominguez D 2005 *Phys. Rev.* B **71** 094521
[9] Nie Q M, Luo M B and Chen Q H 2006 *Phys. Rev.* B **74** 024523
[10] Brito A F, Redinz J A and Plascak J A 2010 *Phys. Rev.* E **81** 031130
[11] Yin J Q, Zheng B and Trimper S 2005 *Phys. Rev.* E **72** 036122
[12] Ozeki Y and Ogawa K 2005 *Phys. Rev.* B **71** 220407
[13] Liu H, Lv J P and Chen Q H 2008 *Europhys. Lett.* **84** 66004
[14] Yotsuyanagi S, Suemitsu Y and Ozeki Y 2009 *Phys. Rev.* E **79** 041138
[15] Prudnikov V V *et al* 2010 *Phys. Rev.* E **81** 011130
[16] Godrèche C and Luck J M 2002 *J. Phys.: Condens. Matter* **14** 1589
[17] Henkel M, Paessens M and Pleimling M 2004 *Phys. Rev.* E **69** 056109
[18] Calabrese P and Gambassi A 2005 *J. Phys. A: Math. Gen.* **38** R133
[19] Lei X W and Zheng B 2007 *Phys. Rev.* E **75** 040104
[20] Walter J C and Chatelain C 2009 *J. Stat. Mech.* P10017
[21] Zhou N J and Zheng B 2008 *Phys. Rev.* E **77** 051104
[22] He Y Y, Zheng B and Zhou N J 2009 *Phys. Rev.* E **79** 021107
[23] Zhou N J, Zheng B and He Y Y 2009 *Phys. Rev.* B **80** 134425
[24] Zhou N J and Zheng B 2010 *Phys. Rev.* E **82** 031139
[25] Schülke L and Zheng B 2000 *Phys. Rev.* E **62** 7482
[26] Monetti R A and Albano E V 2001 *Europhys. Lett.* **56** 400
[27] Loscar E S, Ferrero E E, Grigera T S and Cannas S A 2009 *J. Chem. Phys.* **131** 024120
[28] Albano E V and Saracco G 2002 *Phys. Rev. Lett.* **88** 145701
[29] Lee H K and Okabe Y 2005 *Phys. Rev.* E **71** 015102
[30] Arashiro E, Drugowich de Felicio J R and Hansmanno U H E 2006 *Phys. Rev.* E **73** 040902
[31] Lin S Z and Zheng B 2008 *Phys. Rev.* E **78** 011127
[32] Saracco G P and Gonnella G 2009 *Phys. Rev.* E **80** 051126
[33] Huang X Z, Gong S R, Zhong F and Fan S L 2010 *Phys. Rev.* E **81** 041139
[34] Puzzo M L R and Albano E V 2010 *Phys. Rev.* E **81** 051116
[35] Zhou N J, Zheng B and Landau D P 2010 *Europhys. Lett.* **92** 36001
[36] Fedorenko A A and Trimper S 2006 *Europhys. Lett.* **74** 89
[37] Bray A J, Briant A J and Jervis D K 2000 *Phys. Rev. Lett.* **84** 1503
[38] Chern G W, Youk H and Tchernishyov O 2006 *J. Appl. Phys.* **99** 08Q505
[39] Lua S Y H, Kushvaha S S and Wu Y H *et al* 2008 *Appl. Phys. Lett.* **93** 122504
[40] Nagai T, Yamada H and Konoto M *et al* 2008 *Phys. Rev.* B **78** 180414
[41] Nogawa T and Nemoto K 2009 *Phys. Soc. Japan* **78** 064001
[42] Masseboeuf A, Fruchart O and Toussaint J C *et al* 2010 *Phys. Rev. Lett.* **104** 127204
[43] Gupta R and Baillie C F 1992 *Phys. Rev.* B **45** 2883
[44] Zheng B, Schulz M and Trimper S 1999 *Phys. Rev.* E **59** R1351
[45] Tomita Y and Okabe Y 2002 *Phys. Rev.* B **65** 184405
[46] Bray A J 2000 *Phys. Rev.* E **62** 103
[47] Abriet S and Karevski D 2004 *Eur. Phys. J.* B **37** 47